

AperTO - Archivio Istituzionale Open Access dell'Università di Torino

Modelling the Photochemistry of Imazethapyr in Rice Paddy Water

This is the author's manuscript

Original Citation:

Availability:

This version is available <http://hdl.handle.net/2318/1687086> since 2019-01-17T13:04:42Z

Published version:

DOI:10.1016/j.scitotenv.2018.06.324

Terms of use:

Open Access

Anyone can freely access the full text of works made available as "Open Access". Works made available under a Creative Commons license can be used according to the terms and conditions of said license. Use of all other works requires consent of the right holder (author or publisher) if not exempted from copyright protection by the applicable law.

(Article begins on next page)

Modelling the Photochemistry of Imazethapyr in Rice Paddy Water

Luca Carena^{a*}, Davide Vione^a

^a *Dept. of Chemistry, University of Torino, Via P. Giuria 5, 10125 Turin, Italy*

*Corresponding author:

E-mail address: luca.carena@unito.it

Telephone: +39-011-6705263

Postal address: Via P. Giuria, 5, 10125 Torino, Italy.

Abstract

In this work the photochemistry of imazethapyr, an imidazolinone herbicide used in rice crops, was modelled in rice paddy water. The photochemical half-life time of the herbicide was assessed by means of the APEX software (*Aqueous Photochemistry of Environmentally occurring Xenobiotics*) taking into account the direct photolysis, the reactions with hydroxyl radicals (HO[•]) and, in some cases, the reactions with the excited triplet states of chromophoric dissolved organic matter (³CDOM*). We found that direct photolysis and HO[•] reaction can account for a half-life time ranging between 5 and 11 days in May, which is in quite good agreement with the half-life times measured in the field and reported in the literature. These findings suggest that direct photolysis and reaction with HO[•] are important degradation pathways for imazethapyr in paddy water. Dissolved organic matter (DOM) has been reported in the literature to decrease the imazethapyr photodegradation rate. Our model computations confirm this finding but, upon comparison of model predictions with experimental data from the literature, we provide evidence of a non-negligible role of DOM-photosensitised processes in imazethapyr degradation, particularly in DOM-rich waters. We also assess an upper limit ($1 \times 10^8 \text{ L mol}^{-1} \text{ s}^{-1}$) for the second-order rate constant of the reaction between imazethapyr and ³CDOM*. Furthermore, on the basis of literature-

reported photodegradation pathways and by using both APEX and the US-EPA ECOSAR V2.0 software, we assess that the direct photolysis by-products of imazethapyr could pose a potential ecotoxicological threat to aquatic systems.

Keywords

Imidazolinone herbicides; Photochemical fate; Rice-field water; APEX; Photochemical model.

1. Introduction

Imidazolinone herbicides are pesticides that control a broad spectrum of weeds in different crops, such as rice, wheat and maize (Tan et al., 2005). They inhibit the acetolactate synthase (ALS) enzyme, also called acetohydroxyacid synthase (AHAS), which is a central enzyme in the synthesis of branched-chain amino acids in plants (Lonhienne et al., 2018; Xie et al., 2018). Other ALS-inhibiting herbicides are those belonging to the families of triazolopyrimidines, pyrimidinylthiobenzoates, sulfonylamino-carbonyltriazolinones and sulfonylureas. Imazethapyr, imazapic, imazamox, imazaquin and imazapyr are examples of imidazolinone herbicides (Tan et al., 2005).

The use of pesticides has become indispensable in rice-fields (Wei et al., 2015), and it could increase in the future because of climate change (Rodenburg et al., 2011). The worldwide use of imidazolinone herbicides in paddies is usually associated to the cultivation of imidazolinone-tolerant rice varieties (Sudianto et al., 2013). By applying these herbicides in imidazolinone-tolerant rice crops, it is possible to control the growth of the red rice that causes significant yield losses in rice production (Shivrain et al., 2009). Despite the effectiveness of these herbicides, several works have described the growth of imidazolinone-resistant red rice plants in paddies (Scarabel et al., 2012; Kaloumenos et al., 2013).

The persistence of pesticides in paddies is a problem of environmental concern, because the pesticides occurring in the floodwater can contaminate the surface water bodies connected with the rice fields (Trinh et al., 2014). Previous works have reported the presence of imidazolinone herbicides in the outlet water of rice fields and in surface waters (Battaglin et al., 2000; Milan et al., 2017). The persistence of pesticides is linked to the different degradation pathways that these compounds can undergo in surface waters, including paddy water, such as microbial degradation, chemical hydrolysis and photochemical reactions (Fenner et al., 2013). The latter can be divided into direct photolysis and indirect photochemistry. Direct photolysis occurs when a compound absorbs sunlight and undergoes subsequent transformations, such as bond cleavage or ionisation. In contrast, the indirect phototransformation of a xenobiotic is triggered by reaction with reactive transients species that are usually called Photochemically Produced Reactive Intermediates (PPRIs). The main PPRIs are hydroxyl radicals (HO^\bullet), carbonate radicals ($\text{CO}_3^{\bullet-}$), the excited triplet states of chromophoric dissolved organic matter ($^3\text{CDOM}^*$) and singlet oxygen ($^1\text{O}_2$). They are formed upon sunlight absorption by photosensitisers (CDOM, nitrate and nitrite) that occur naturally in surface water bodies. All of the mentioned photosensitisers are directly involved in the formation of HO^\bullet radicals, and they also indirectly produce $\text{CO}_3^{\bullet-}$ through the oxidation of bicarbonate and carbonate by photogenerated HO^\bullet (to a lesser extent, $\text{CO}_3^{\bullet-}$ is also produced upon carbonate oxidation by $^3\text{CDOM}^*$) (Buxton et al., 1988; Mack and Bolton, 1999; Canonica et al., 2005). DOM is the main scavenger of HO^\bullet and $\text{CO}_3^{\bullet-}$ and, therefore, the associated photoprocesses are usually enhanced in DOM-poor waters (Vione et al., 2014). CDOM under irradiation is also the source of $^3\text{CDOM}^*$ and $^1\text{O}_2$, where the latter is formed by energy transfer processes between $^3\text{CDOM}^*$ and ground-state molecular oxygen (Haag and Hoigné, 1986; Appiani and McNeill, 2015; McNeill and Canonica, 2016). The processes triggered by $^3\text{CDOM}^*$ and $^1\text{O}_2$ are usually favoured in DOM-rich waters (Vione et al., 2014).

Photochemical reactions can be important degradation pathways for many pesticides in surface waters, including the imidazolinone herbicides (Mabury and Crosby, 1996; Armbrust, 2000;

Burrows et al., 2002; Remucal, 2014). Specifically, in the case of imazethapyr, [5-ethyl-2-(4-isopropyl-4-methyl-5-oxo-4,5-dihydroimidazol-1H-2-yl)nicotinic acid], the photochemical transformations prevail over chemical hydrolysis (Ramezani et al., 2008). Imazethapyr has been found to degrade by direct photolysis and with HO[•] radicals (Avila et al., 2006). The presence of DOM has been reported to decrease the imazethapyr degradation rate because of light screening (Elazzouzi et al., 2002; Ramezani et al., 2008; Espy et al., 2011). In this work, the photochemical fate of imazethapyr (half-life times, role of direct photolysis and PPRIs in photodegradation) was modelled in rice-field water by using a suitable photochemistry-modelling software (APEX; Bodrato and Vione, 2014), on the basis of herbicide photochemical parameters from the literature and of data from a previous study into the photoreactivity of paddy-field CDOM (Carena et al., 2017). Furthermore, a rough assessment of the reactivity of imazethapyr toward ³CDOM* was carried out in this work by comparing literature data with our model predictions. Finally, some toxicological features of the imazethapyr phototransformation products were assessed based on literature-reported degradation pathways and by using Structure-Activity Relationships software (ECOSAR V2.0), developed by US-EPA.

2. Materials and Methods

2.1 Photochemical Modelling

The photochemical modelling was carried out with the APEX software (*Aqueous Photochemistry of Environmentally occurring Xenobiotics*) (Bodrato and Vione, 2014). APEX is a suitable modelling tool that has been used in several previous works to assess the photochemical fate of xenobiotics in well mixed surface-waters, in which the chemical composition profile can be considered constant with the water depth (see, e.g., Vione, 2014). A detailed description of the APEX mathematical model is explained in the software User's Guide, which is freely available as supporting information in Bodrato and Vione (2014). Briefly, APEX requires input data concerning the

photoreactivity of both the studied xenobiotic (namely, the direct photolysis quantum yield and the second-order rate constants for reaction with the PPRIs) and the surface-water environment. The imazethapyr photolysis quantum yield and its second-order rate constant for reaction with HO[•] have been measured by Avila et al. (2006) as 0.023 and $2.8 \times 10^{13} \text{ L mol}^{-1} \text{ h}^{-1}$ (i.e., $7.8 \times 10^9 \text{ L mol}^{-1} \text{ s}^{-1}$), respectively. We used these values to model the photochemical fate of imazethapyr. The cited authors have performed irradiation experiments with a simulated sunlight equipment and have measured the imazethapyr direct photolysis quantum yield and the HO[•]-reaction rate constant by comparing the herbicide photodegradation with that of a chemical actinometer and of reference compounds, respectively.

The water chemical composition is a key environmental feature for phototransformation, because water chemistry and photochemistry are closely connected. In particular, the concentrations of DOM (expressed as dissolved organic carbon, DOC), nitrate, nitrite, bicarbonate and carbonate are key input data to assess the photochemical fate of a xenobiotic by using APEX. Other very important environmental parameters are the depth of the water body, the sunlight spectrum and the absorption spectrum of the water itself (which is mainly accounted for by CDOM and is modelled by APEX based on the DOC value). Because the photochemical processes are enhanced in clear and shallow water bodies, the photochemical half-life times can be highly affected by the water depth (Beretvas et al., 2000). The standard spectral photon flux densities used in APEX are referred to a sunlight spectrum reaching the water surface in a cloudless 15th July at 45°N latitude, at 9 am or 3 pm solar time, with a UV-irradiance of 22 W m^{-2} . The total amount of sunlight energy reaching the ground in one such day defines the Summer Sunny Day (SSD) time unit used in the model, which is equivalent to a mid-latitude, fair-weather 15 July and corresponds to 10 h of continuous irradiation at steady 22 W m^{-2} UV irradiance. Finally, the formation quantum yields of the PPRIs HO[•], ³CDOM* and ¹O₂ by irradiated CDOM (respectively, $\Phi_{HO^{\bullet}}^{CDOM}$, $\Phi_{^3CDOM^*}^{CDOM}$ and $\Phi_{^1O_2}^{CDOM}$) are key input parameters of the model, and they depend upon the considered environment. Several previous

works have photochemically characterised sunlit aquatic environments such as, for instance, lakes and paddy floodwater (Canonica et al., 2005; Al Housari et al., 2010; Timko et al., 2014; Carena et al., 2017). Paddy-water photoreactivity parameters are available from Carena et al. (2017), who report $\Phi_{HO^\bullet}^{CDOM} = 2.3 \times 10^{-5}$, $\Phi_{^3CDOM^*}^{CDOM} = 2.9 \times 10^{-2}$, and $\Phi_{^1O_2}^{CDOM} = 9.0 \times 10^{-3}$.

In this work, the photochemical fate of imazethapyr was modelled in a typical environment (water depth = 5 cm) of a paddy field located at northern mid-latitude during the first half of May, at the beginning of the rice growing season. This is a period when the rice-fields are flooded, their water depth can range between 5 and 15 cm and the rice plants are still in their early growth stages (Roger, 1996), thus the sunlight shadowing by the rice-plant canopy can be neglected (Carena and Vione, 2017). We fixed the water depth equal to 5 cm without considering fluctuations due to dynamic hydrological events such as irrigation, rainfall, evapotranspiration and percolation. Although water depth can highly affect the photochemical processes (Beretvas et al., 2000), rice-field water is a shallow aquatic system where absorption saturation is unlikely to occur. Therefore, one expects little variations of the model results when changing the depth between 5 and 15 cm and by taking constant the water chemical composition. The dissolved organic carbon (DOC) and nitrate content were used as master variables to assess the photochemical fate of imazethapyr, because direct photolysis and the reactivity with HO^\bullet radicals are generally influenced by these two parameters (Vione et al., 2014). Based on literature reports (Quesada et al., 1997; Barreiros et al., 2011; Carena et al., 2017), DOC values between 4 and 10 mgC L⁻¹ and nitrate concentrations between 1.5 and 100 $\mu\text{mol L}^{-1}$ are reasonable for paddy floodwater. The used bicarbonate and carbonate concentrations were computed by taking into account an air-equilibrated aqueous system at pH 8 (25 °C, 3 mmol L⁻¹ ionic strength), and they were $[\text{HCO}_3^-] = 6.8 \times 10^{-4} \text{ mol L}^{-1}$ and $[\text{CO}_3^{2-}] = 4.0 \times 10^{-6} \text{ mol L}^{-1}$, respectively. However, bicarbonate and carbonate concentrations could be quite far from these values because the paddy-field system can undergo both diurnal and longer-term pH fluctuations due to the photosynthetic processes taking place in the floodwater (Roger, 1996) and to

the exchange of CO₂ between air, water and soil (Saito and Watanabe, 1978). Although inorganic carbon can affect the photochemistry of CO₃^{•-}-reactive compounds (Huang and Mabury, 2000; Liu et al., 2016), to our knowledge this is not the case of imazethapyr.

The July-based APEX output data were converted into May-based ones by means of the *APEX_season* function, which basically makes a correction for the incident solar irradiance. Furthermore, the optical depth of the floodwater (6 cm) was computed by correcting the actual depth (5 cm) for a 1.2 factor that takes into account both the solar zenith angle and the refraction of light at the air-water interface (Bodrato and Vione, 2014; Carena and Vione, 2017).

2.2 Toxicological modelling

Acute-toxicity parameters (LC₅₀ and EC₅₀) and chronic toxicity values (ChV) to aquatic organisms were assessed by using the ECOSAR V2.0 software [Ecological Structure Activity Relationships (ECOSAR) Class Program], developed by the U.S. Environmental Protection Agency (EPA) and freely available (<https://www.epa.gov/tsca-screening-tools/ecological-structure-activity-relationships-ecosar-predictive-model>; Mayo-Bean et al., 2012). Several previous studies have used U.S. EPA ECOSAR to predict aquatic toxicity of chemicals (Reuschenbach et al., 2008; Frank et al., 2010; Ortiz de García et al., 2014). The software can assess also other chemical properties, such as the water solubility. Here, the LC₅₀ and EC₅₀ values higher than the predicted water solubility of the relevant compounds were neglected.

3. Results and Discussion

3.1. Photodegradation by direct photolysis and HO^\bullet reaction

Fig.1 shows the computed photochemical half-life times ($t_{1/2}$) of imazethapyr in rice-field water as a result of direct photolysis and HO^\bullet reaction, as a function of the DOC that measures DOM. We find that DOM affects the photodegradation of imazethapyr by increasing its $t_{1/2}$ value, in agreement with reports from the literature (Elazzouzi et al., 2002; Ramezani et al., 2008; Espy et al., 2011). At $DOC \sim 5 \text{ mgC L}^{-1}$, the modelled pesticide $t_{1/2}$ in May ranges between 8 and 11 days but faster photodegradation can occur at lower DOC. These results are in reasonable agreement with the reported lifetime of 3-7 days for imazethapyr in the field (Santos et al., 2008; Zanella et al., 2011; Martini et al., 2013; Reimche et al., 2015). Furthermore, Reimche et al. (2015) have measured $t_{1/2} \sim 5$ days in subtropical rice-field water, suggesting that photodecomposition is the main imazethapyr breakdown process in such an environment. Similar results have been found by Santos et al. (2008).

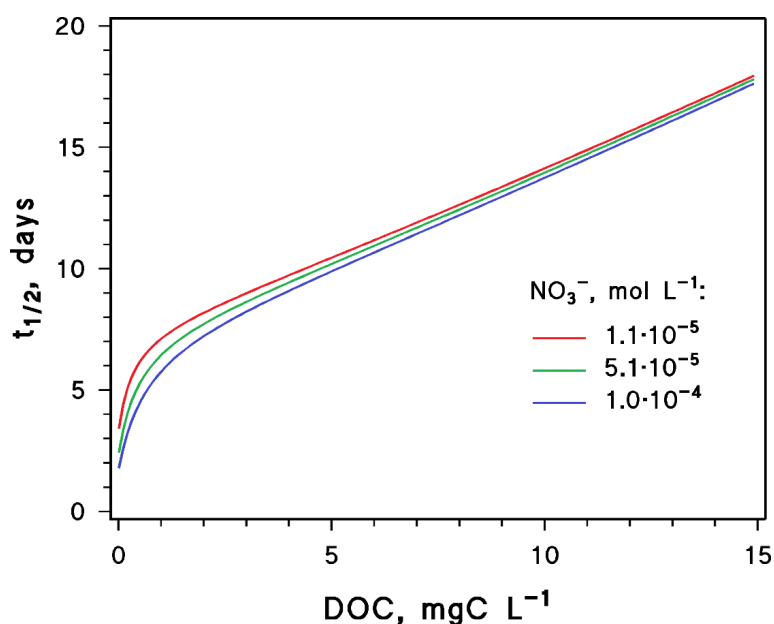


Fig. 1. Photochemical half-life times of imazethapyr in paddy-field water computed with APEX, as a function of water DOC and for different nitrate levels. Direct photolysis and reactions with hydroxyl radicals account for the pesticide photodegradation. Other APEX input data were as follows: $1.5 \times 10^{-6} \text{ mol L}^{-1} NO_2^-$, $6.8 \times 10^{-4} \text{ mol L}^{-1} HCO_3^-$, $4.0 \times 10^{-6} \text{ mol L}^{-1} CO_3^{2-}$ and 6 cm optical depth.

Nitrate affects the half-life time of the pesticide, especially at low DOC values where the HO[•] radicals play an important role in the overall photodegradation (see Fig.2 for the DOC trend of the imazethapyr photoreaction pathways). Actually, nitrate is a HO[•] source (and the main one at low DOC, together with nitrite) while DOM is the main scavenger (Vione et al., 2014), which accounts for the favourable role of nitrate towards photodegradation (the role of HO[•] at low DOC is more important if nitrate is more concentrated, see Fig.2). The scavenging of HO[•] by DOM is one of the reasons why the photoreaction kinetics of imazethapyr get slower as the DOC increases (see Fig.1).

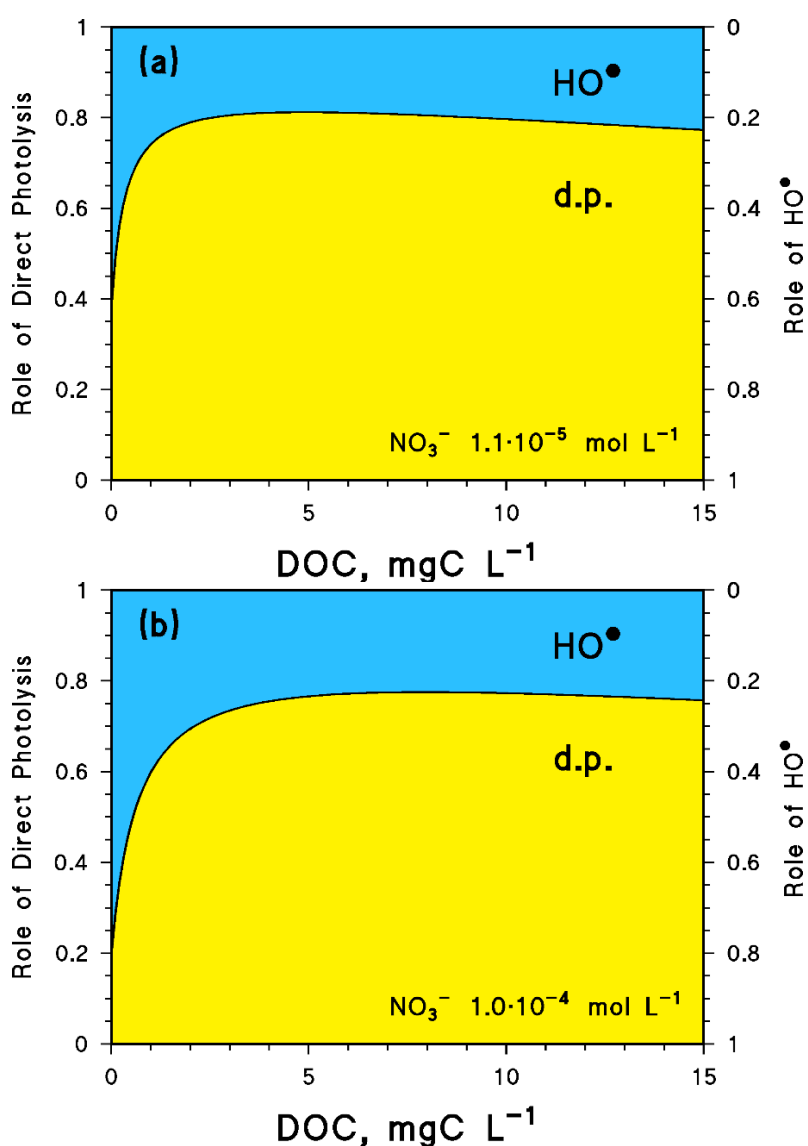


Fig. 2. Role of direct photolysis and hydroxyl radicals reactions in the overall photodegradation of imazethapyr in paddy water, at different nitrate concentrations. The curves were computed with the APEX software. Other APEX input data were as follows: $1.5 \times 10^{-6} \text{ mol L}^{-1} \text{ NO}_2^-$, $6.8 \times 10^{-4} \text{ mol L}^{-1} \text{ HCO}_3^-$, $4.0 \times 10^{-6} \text{ mol L}^{-1} \text{ CO}_3^{2-}$ and 6 cm optical depth.

In contrast, the role of nitrate on pesticide photodegradation and the effect of its concentration become very small at relatively high DOC levels ($> 5 \text{ mgC L}^{-1}$), where there is little difference in the $t_{1/2}$ values with varying nitrate (see Fig.1). At high DOC the DOM is an efficient HO^\bullet scavenger (which favours imazethapyr phototransformation by direct photolysis, see Fig.2) and CDOM becomes the main HO^\bullet source, thus an increase in the nitrate content cannot affect much the photoreaction kinetics.

3.2. An assessment of the role of $^3\text{CDOM}^*$ in imazethapyr photodegradation

The DOC is a key variable affecting the half-life of imazethapyr, which becomes longer as the DOC increases (Fig.1). There are two main reasons for this finding, namely: (i) the screening effect of CDOM, which absorbs sunlight and inhibits the imazethapyr direct photolysis, and (ii) the HO^\bullet radicals scavenging (note that both direct photolysis and HO^\bullet reactions are inhibited as the DOC increases, but the HO^\bullet processes are inhibited to a higher extent; Vione et al., 2014). Coherently, previous works have shown that natural organic matter (NOM) decreases the photodegradation rate of imazethapyr (Elazzouzi et al., 2002; Ramezani et al., 2008; Espy et al., 2011). However, in spite of these experimental evidences corroborated by model calculations, CDOM could still act as a photosensitiser for the degradation of imazethapyr at high DOC values. Such a result has for instance been reported in the case of triclosan (Bianco et al., 2015), where phototransformation is slowed down upon addition of CDOM but is dominated by $^3\text{CDOM}^*$ at high DOC. It is thus interesting to assess a possible reactivity of imazethapyr toward $^3\text{CDOM}^*$, also because paddy fields are photochemical reactors where $^3\text{CDOM}^*$ potentially play an important role (Carena et al., 2017). Espy et al. (2011) have assessed the effect of natural organic matter (NOM) on imazethapyr photodegradation with outdoor photolysis experiments (July, $\sim 44^\circ\text{N}$ latitude). In that study, imazethapyr has been irradiated in phosphate-buffered (pH 7) ultrapure-water solutions in the presence of Suwannee River NOM (52.5% C by mass). The (pseudo-first order) rate constant of imazethapyr photodegradation (k') has been shown to decrease, compared to that in buffered ultra-

pure water, by ~20% at both 1.6 and 5.0 mg L⁻¹ NOM, and by ~33% at 9.2 mg L⁻¹ NOM (corresponding to ~0.84, 2.60 and 4.83 mgC L⁻¹ DOC, respectively). By using APEX, we roughly assessed the second-order reaction rate constant between imazethapyr and ³CDOM* (k_I^{T*}), by reproducing the DOC trend of the ratio $k'_{DOCj} (k'_{DOC0})^{-1}$ obtained from the data reported by Espy et al. (2011). Here, k'_{DOCj} is the pseudo-first order transformation rate constant of imazethapyr in the presence of j mgC L⁻¹ DOC, whereas k'_{DOC0} refers to low to nil DOC content.

To better simulate the experimental conditions of Espy et al. (2011), we adopted low concentration of nitrate and negligible (1×10^{-10} mol L⁻¹) nitrite levels. The bicarbonate and carbonate concentrations were computed by taking into account an air-equilibrated water system at pH 7. Note that these water conditions are completely different from those used to model the imazethapyr photochemical fate in paddy-water, because in this case was had to model the photochemical behaviour of synthetic solutions. Furthermore, we used physical-chemical features of typical (C)DOM that occur in rivers and lakes (Bodrato and Vione, 2014), rather than the (C)DOM of the paddy-water environment. For instance, we used PPRIs formation quantum yields $\Phi_{HO\cdot}^{CDOM} = 3 \times 10^{-5}$, $\Phi_{^3CDOM*}^{CDOM} = 1.3 \times 10^{-3}$ and $\Phi_{^1O_2}^{CDOM} = 1.2 \times 10^{-3}$. Fig.3 shows the literature experimental data, superposed to the $k'_{DOCj} (k'_{DOC0})^{-1}$ curves modelled with APEX for different values of k_I^{T*} . A good fit of the experimental data of Espy et al. (2011) was achieved by assuming 3×10^{-7} mol L⁻¹ NO₃⁻ and $k_I^{T*} = 1 \times 10^8$ L mol⁻¹ s⁻¹. The literature data could be reproduced reasonably well also by assuming $k_I^{T*} = 10^6$ - 10^7 L mol⁻¹ s⁻¹. In contrast, $k_I^{T*} > 10^8$ L mol⁻¹ s⁻¹ produced a notable increase of $k'_{DOCj} (k'_{DOC0})^{-1}$ with increasing DOC, especially above 1 mgC L⁻¹, because of a considerable reactivity between imazethapyr and ³CDOM*. Note that ¹O₂, which is formed as a consequence of ³CDOM* production, was not taken into account because it is often poorly reactive toward xenobiotic compounds (Vione et al., 2014). For the above reasons, $k_I^{T*} = 10^8$ L mol⁻¹ s⁻¹ could be considered as an upper limit for the reaction rate constant between imazethapyr and ³CDOM*.

However, further experimental studies should be carried out to better understand the reactivity between imazethapyr and $^3\text{CDOM}^*$, by using, for instance, CDOM-proxy compounds such as anthraquinone-2-sulphonate (AQ2S) or 4-carboxybenzophenone (CBBP) (Minella et al., 2018).

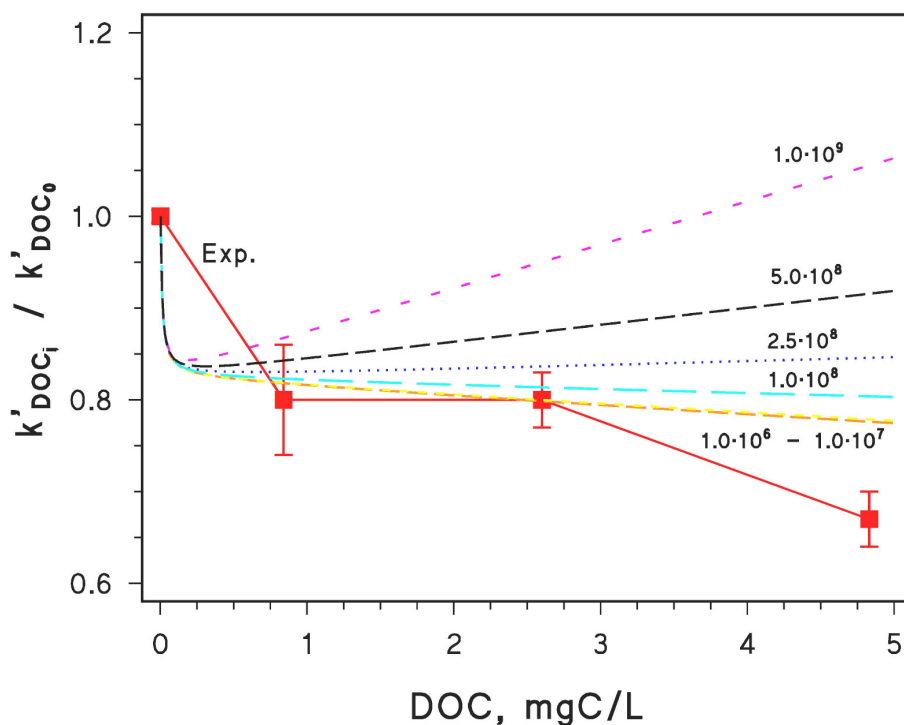
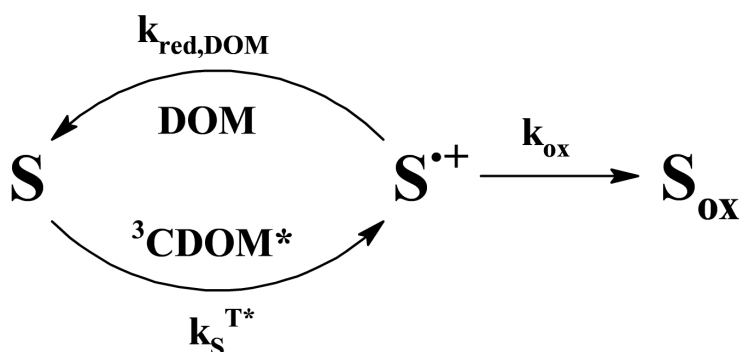


Fig. 3. Model reproduction of the experimental data (■) reported by Espy et al. (2011), with the associated error bounds ($\pm \sigma$). The curves were computed at different values of k'_I by using the APEX software. Other APEX input data were as follows: $3 \times 10^{-7} \text{ mol L}^{-1} \text{ NO}_3^-$, $1 \times 10^{-10} \text{ mol L}^{-1} \text{ NO}_2^-$, $5.6 \times 10^{-5} \text{ mol L}^{-1} \text{ HCO}_3^-$, $3.7 \times 10^{-8} \text{ mol L}^{-1} \text{ CO}_3^{2-}$ and 3 cm optical path length.

The partial mismatch between model predictions and experimental data at DOC around 5 mgC L^{-1} (see Fig.3) could be accounted for in part by the (shown) uncertainty in the experimental data, and in part by the model relative error of about 10-20%. Moreover, differences between the photochemical features of the experimental CDOM and those assumed in the model could account for different photoreaction kinetics. Finally, it must be pointed out that our model did not include the possible back-reduction effects that can be operational in the case of several xenobiotics

(Canonica and Laubscher, 2008), where the DOM phenolic moieties reduce back to the initial compound the radical species produced by oxidation of the substrate by $^3\text{CDOM}^*$ (Scheme 1; Wenk et al., 2011; Wenk and Canonica, 2012; Yuan et al., 2016). Such an effect could account for the photoreactivity decrease at high DOC.



Scheme 1. Back-reduction effect leading to the inhibition of the oxidation of the substrate S by $^3\text{CDOM}^*$ (adapted from Wenk et al., 2011).

The reaction between imazethapyr and $^3\text{CDOM}^*$ could modify the predicted herbicide half-lives in paddy water. To take the $^3\text{CDOM}^*$ role into account, Fig.4a shows the herbicide half-life times for different values of k_l^{T*} (the values of $k_l^{T*} > 10^8 \text{ L mol}^{-1} \text{ s}^{-1}$ are only included as examples). The model conditions are here referred to paddy water and not to ultra-pure water. Note that, if $k_l^{T*} \leq 10^6 \text{ L mol}^{-1} \text{ s}^{-1}$, $t_{1/2}$ would not change significantly as compared to the scenario reported in Fig.1. In such a case, the reactions with $^3\text{CDOM}^*$ have unimportant role in the overall degradation of the herbicide, which is dominated by direct photolysis and HO^\bullet reaction (see Fig.5a for the main pathways of imazethapyr photodegradation with $k_l^{T*} = 10^6 \text{ L mol}^{-1} \text{ s}^{-1}$). However, by increasing k_l^{T*} by an order of magnitude ($k_l^{T*} = 10^7 \text{ L mol}^{-1} \text{ s}^{-1}$), one has a significant role of the $^3\text{CDOM}^*$

process for $\text{DOC} > 3 \text{ mgC L}^{-1}$ (see Fig.5b). The $t_{1/2}$ vs. DOC curve gets modified as a consequence (see the relevant curve in Fig.4a, and compare it with the corresponding curve in Fig.1). The pseudo-plateau (actually, a broad maximum) observed for $t_{1/2}$ as a function of the DOC, for $k_I^{T^*} = 10^7 \text{ L mol}^{-1} \text{ s}^{-1}$ and $\text{DOC} > 3 \text{ mgC L}^{-1}$, is accounted for by the fact that the inhibition of the direct photolysis and of the HO^\bullet -induced degradation of imazethapyr is counterbalanced by the reaction with $^3\text{CDOM}^*$ (Fig.5b).

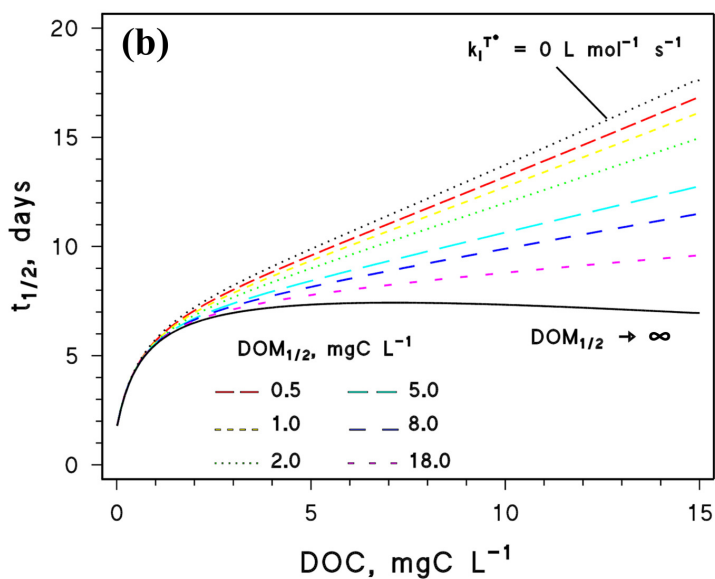
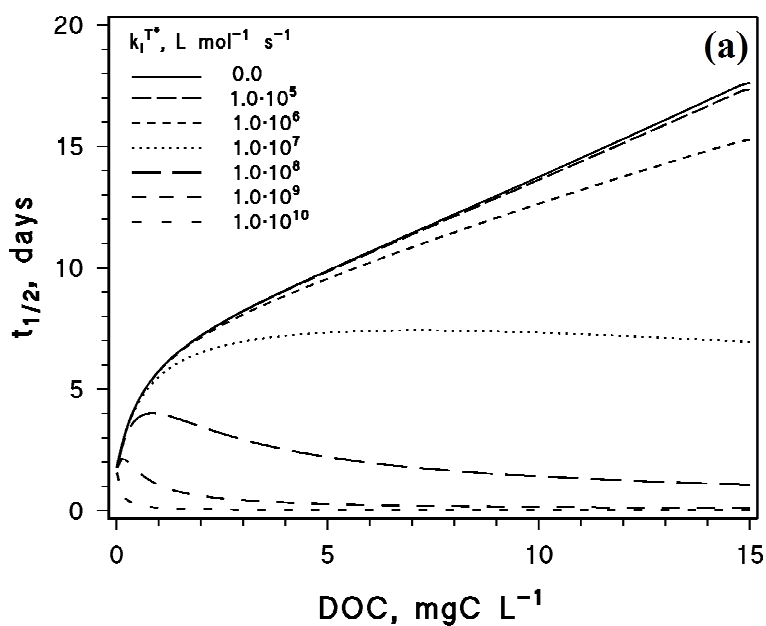


Fig. 4. Half-life times of imazethapyr in paddy floodwater, for (a) different values of k_I^{T*} and (b) different values of $DOM_{1/2}$ ($k_I^{T*} = 1.0 \times 10^7 \text{ L mol}^{-1} \text{ s}^{-1}$). Other APEX input data were as follows: $1.0 \times 10^{-4} \text{ mol L}^{-1} \text{ NO}_3^-$, $1.5 \times 10^{-6} \text{ mol L}^{-1} \text{ NO}_2^-$, $6.8 \times 10^{-4} \text{ mol L}^{-1} \text{ HCO}_3^-$, $4.0 \times 10^{-6} \text{ mol L}^{-1} \text{ CO}_3^{2-}$ and 6 cm optical depth.

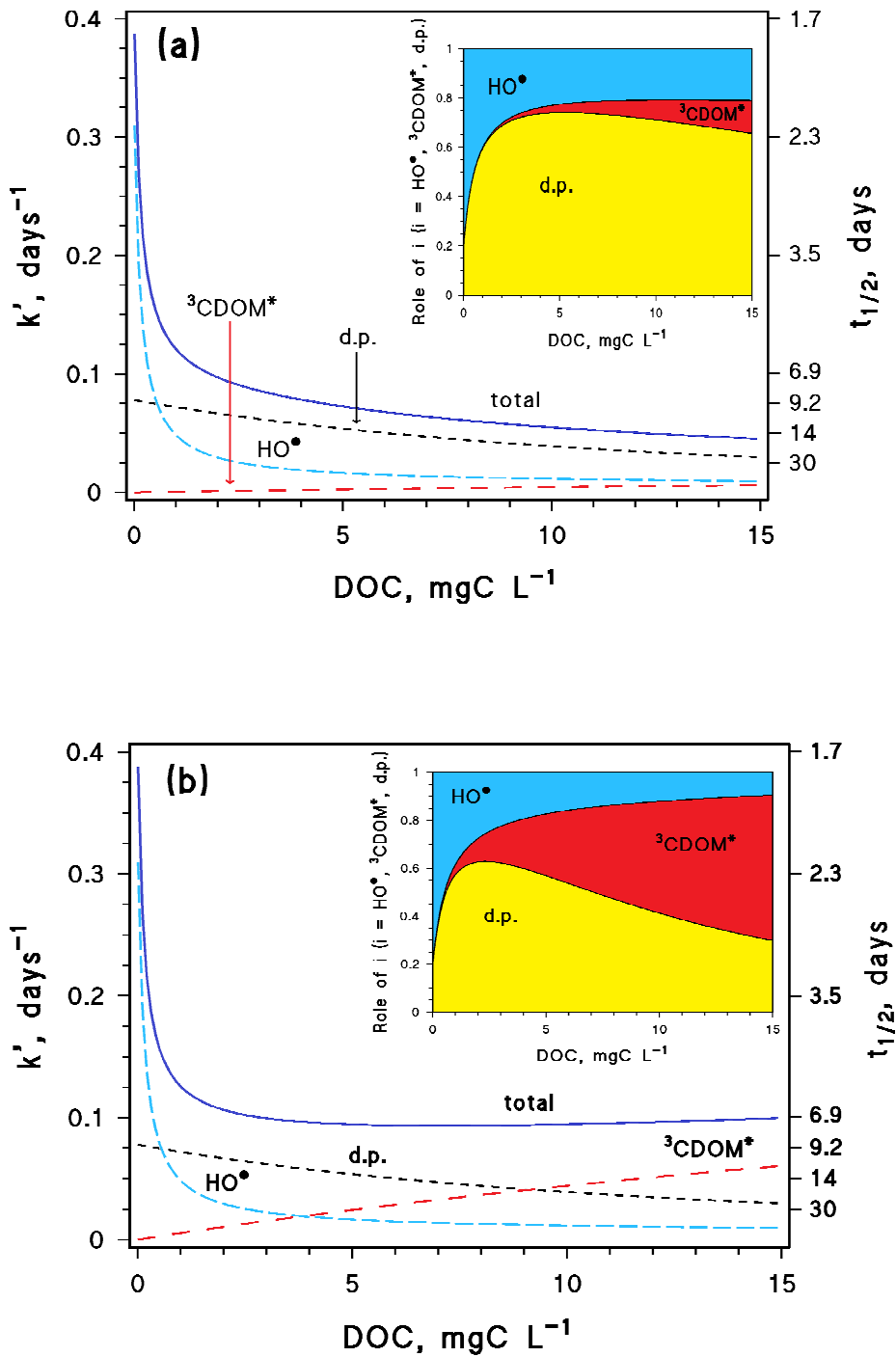


Fig. 5. Pseudo-first order rate constants ($k'_{d,p}$, k'_{HO^\bullet} , k'_{3CDOM^*} , and $k'_{total} = k'_{d,p} + k'_{HO^\bullet} + k'_{3CDOM^*}$) of imazethapyr photodegradation in paddy floodwater. The used $k_I^{T^*}$ values were (a) $1.0 \times 10^6 \text{ L mol}^{-1} \text{ s}^{-1}$ and (b) $1.0 \times 10^7 \text{ L mol}^{-1} \text{ s}^{-1}$. Other APEX input data were as follows: $1.0 \times 10^{-4} \text{ mol L}^{-1} \text{ NO}_3^-$, $1.5 \times 10^{-6} \text{ mol L}^{-1} \text{ NO}_2^-$, $6.8 \times 10^{-4} \text{ mol L}^{-1} \text{ HCO}_3^-$, $4.0 \times 10^{-6} \text{ mol L}^{-1} \text{ CO}_3^{2-}$ and 6 cm optical depth. The inserts show the fractions of imazethapyr photodegradation accounted for by the different photoreaction pathways.

The predicted half-lives for $k_I^{T^*} = 10^7 \text{ L mol}^{-1} \text{ s}^{-1}$ and DOC around 5 mgC L^{-1} (about one week) are still compatible with the literature reports (Santos et al., 2008; Zanella et al., 2011; Reimche et al., 2015), and the agreement is even better than for the case when the $^3\text{CDOM}^*$ reactions were neglected. While not making conclusive evidence in favour of a significant $^3\text{CDOM}^*$ reaction, this means anyway that the literature data suggest $k_I^{T^*} \leq 10^8 \text{ L mol}^{-1} \text{ s}^{-1}$ and, possibly, $k_I^{T^*} \sim 10^7 \text{ L mol}^{-1} \text{ s}^{-1}$.

Although to our knowledge a possible back-reduction effect on imazethapyr oxidation by $^3\text{CDOM}^*$ has not yet been investigated, we tried to include it into the model. Of course this operation implies a certain degree of speculation, but it can show how the back-reduction process might affect the imazethapyr photodegradation if it were operational. Furthermore, paddy-water DOM is mainly composed by soil-derived humic substances (Carena et al., 2017) that can act as effective anti-oxidants (Wenk et al., 2011; Vione et al., 2018). Fig.4b shows the photochemical lifetimes for different values of $\text{DOM}_{1/2}$, which measures the back-reduction effect. $\text{DOM}_{1/2} = k_{ox} (k_{red,DOM})^{-1}$ does in fact represent the DOC value that halves the photodegradation rate constant by $^3\text{CDOM}^*$, compared to the case when the back-reduction is not operational (Canonica and Laubscher, 2008). The lower is $\text{DOM}_{1/2}$, the more important are the back-reduction reactions. In general, $\text{DOM}_{1/2}$ depends upon the type of DOM and the xenobiotic and previous studies have shown that it can vary between 0.7 and 17 mgC L^{-1} (Canonica and Laubscher, 2008; Vione et al., 2018). By assuming $k_I^{T^*} = 10^7 \text{ L mol}^{-1} \text{ s}^{-1}$, one can take into account the inhibition of the xenobiotic oxidation by $^3\text{CDOM}^*$

by using an apparent reaction rate constant that is expressed as the product ψk_I^{T*} . Here, $\psi = [1 + \text{DOC} \cdot (\text{DOM}_{1/2})^{-1}]^{-1}$ takes into account the back-reduction effect (Vione et al, 2018). Indeed, by assuming $\text{DOM}_{1/2} = 0.5 \text{ mgC L}^{-1}$ (i.e., important back reactions), the half-life times approach those computed without including the reactivity of imazethapyr with $^3\text{CDOM}^*$ (that is, $k_I^{T*} = 0 \text{ L mol}^{-1} \text{ s}^{-1}$). In contrast, by assuming higher $\text{DOM}_{1/2}$ values that imply a lower importance of the back reduction, the half-lives become increasingly similar to those observed in the case of no back-reduction.

3.3. Assessment of the possible toxicity of the known direct-photolysis intermediates of imazethapyr, and of the conditions that would enhance their occurrence in the environment

As shown in Fig.5, direct photolysis is a non-negligible transformation pathway for imazethapyr, even at quite high DOC levels. Espy et al. (2011) have proposed mechanistic pathways for the direct photolysis of imazethapyr at $\sim 254 \text{ nm}$. Although this wavelength is not environmentally significant, it has been suggested that the mechanism could be similar in the environment. Actually, Kasha's rule for the fate of the excited states suggests that relatively complex organic molecules may have direct photolysis quantum yields and pathways that poorly depend on the irradiation wavelengths (Turro et al., 1978).

Moreover, previous works have reported similar degradation pathways for the direct photolysis at wavelengths $> 290 \text{ nm}$ of other imidazolinone herbicides, with comparable molecular structure as imazethapyr (Quivet et al., 2004; Quivet et al., 2006; Harir et al., 2007; Christiansen et al., 2015). It is thus possible and interesting to assess the possible impacts on the aquatic environment of the known imazethapyr phototransformation products. By using the ECOSAR V2.0 software, we estimated both short-term and chronic aquatic toxicology data. Fig.6 shows the acute toxicity to aquatic organisms (fish, daphnid and algae) of the direct photolysis by-products of imazethapyr,

identified by Espy et al. (2011) and here indicated with the same acronyms used in the original paper (P1 to P6). The compounds P4, P3, P5b and P5a are directly formed upon imazethapyr direct photolysis, while P2 and P1 derive from P4 and P3, respectively, and P6 derives from P5a. The predicted toxicological data suggest that the compounds P1 to P4 could produce an increase of the acute toxicity to aquatic organisms (with ECOSAR, two compounds can be said to have different toxicity if the predicted values differ by at least one order of magnitude, i.e., one logarithmic unit in the plot of Fig.6; Mayo-Bean et al., 2012). The toxicity of the other by-products (P5a, P5b, P6) would be comparable to or lower than that of imazethapyr. A similar trend was found for the chronic toxicity (data not shown) as assessed by means of the Chronic Value (ChV) parameter, which is the geometric mean of the NOEC and LOEC values (No/Lowest Observed Effect Concentration, respectively; Mayo-Bean et al., 2012).

Because of the potential formation of more toxic compounds, the direct photolysis of imazethapyr could be of environmental concern. It is thus important to assess the conditions where the direct photolysis is an important degradation pathway for imazethapyr, and where its kinetics is fast enough. Fig.7a shows that direct photolysis would be the fastest at low DOC. However, under such conditions the HO[•] reaction would be an important competing pathway. As shown in Fig.7b, the role of the imazethapyr direct photolysis would be enhanced when DOC ~ 2 mgC L⁻¹, and it would be important even above that value if $k_t^{T*} < 10^7 \text{ L mol}^{-1} \text{ s}^{-1}$. In the other cases, the relative importance of the direct photolysis would be decreased by the competition of HO[•] and ³CDOM* reactions. Overall, one could expect significant photoproduction of toxic direct photolysis by-products at intermediate DOC levels (e.g., 2-5 mgC L⁻¹). However, a more precise estimate of the impact of imazethapyr direct photolysis on aquatic organisms requires the knowledge of the formation yields of the toxic by-products, which are presently unavailable.

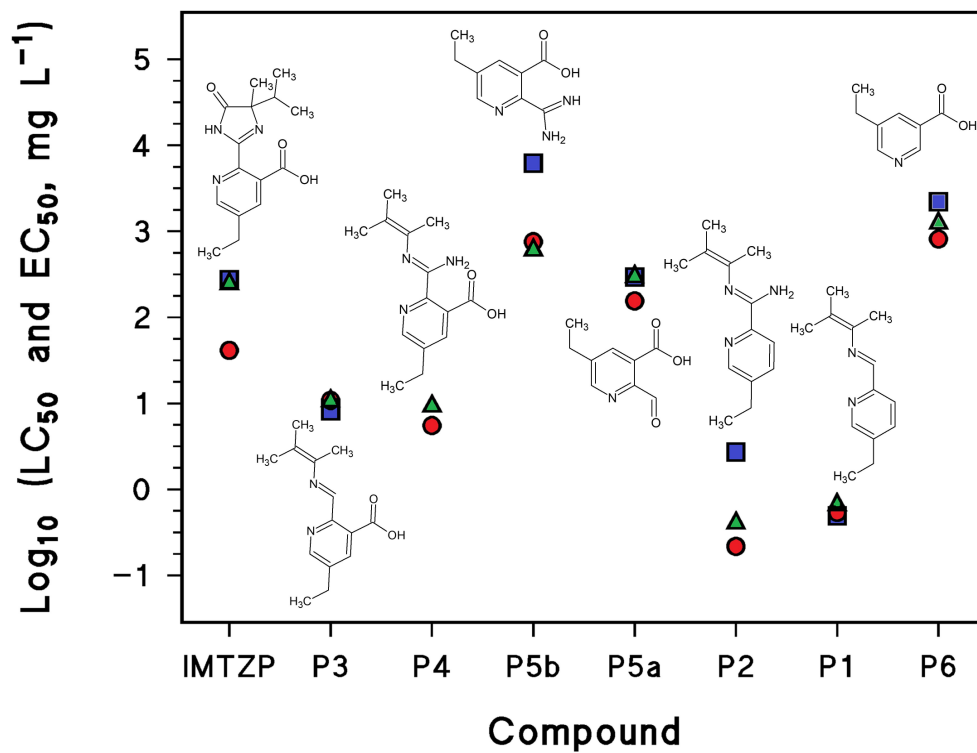


Fig. 6. Acute-toxicity data computed with the ECOSAR V2.0 software (US-EPA) for the compounds formed upon imazethapyr direct photolysis (Espy et al., 2011). Note the logarithmic scale on the Y-axis. Also note that LC₅₀ refers to fish (96 h, ■) and daphnid (48 h, ▲), while EC₅₀ refers to green algae (96 h, ●). IMTZP = imazethapyr.

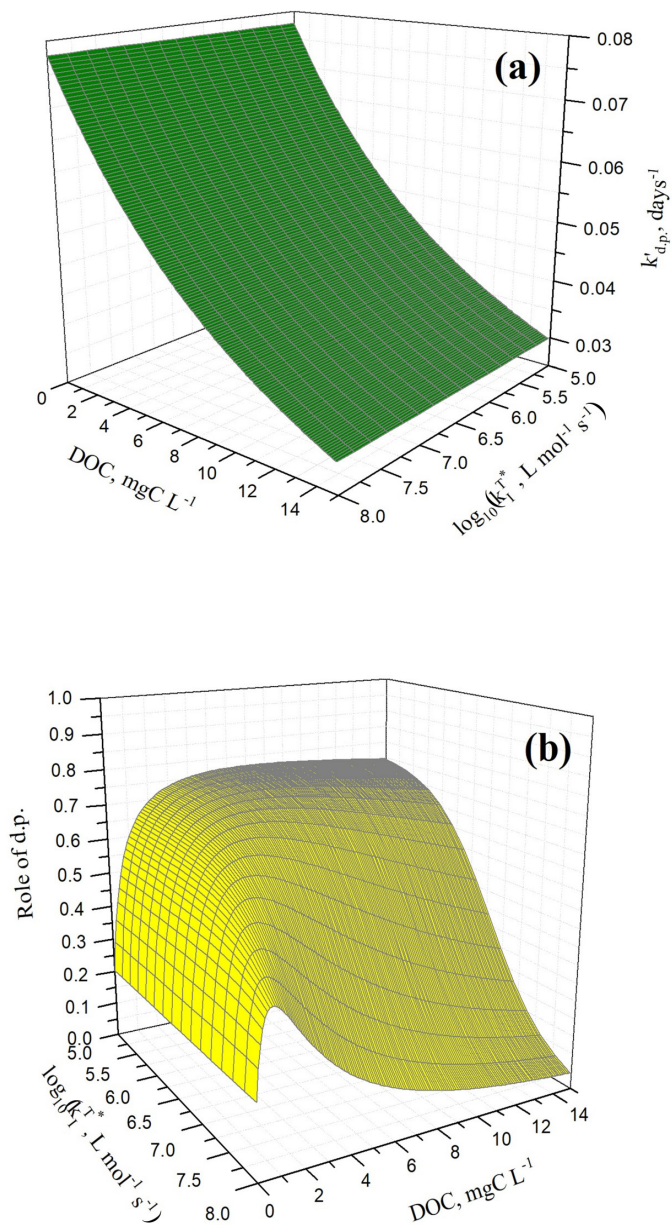


Fig. 7. (a) Imazethapyr direct photolysis pseudo-first order rate constant and (b) role of direct photolysis in the overall herbicide photodegradation in paddy water (May), as a function of the DOC and of the decimal logarithm of the second-order reaction rate constant between imazethapyr and $^3\text{CDOM}^*$. The curves were computed with the APEX software. Relevant APEX input data were as follows: $1.0 \times 10^{-4} \text{ mol L}^{-1} \text{ NO}_3^-$, $1.5 \times 10^{-6} \text{ mol L}^{-1} \text{ NO}_2^-$, $6.8 \times 10^{-4} \text{ mol L}^{-1} \text{ HCO}_3^-$, $4.0 \times 10^{-6} \text{ mol L}^{-1} \text{ CO}_3^{2-}$ and 6 cm optical depth.

4. Conclusions

Previous works have demonstrated that (i) imazethapyr undergoes relatively fast phototransformation in aqueous solution by direct photolysis and HO[•] reaction (Avila et al., 2006), and (ii) it has a half-life time in paddy water ranging between 3 and 7 days (Santos et al., 2008; Zanella et al., 2011; Martini et al., 2013; Reimche et al., 2015). In this study, the photochemical fate of imazethapyr was modelled in paddy floodwater by using the APEX software. The half-life time was first computed by taking into account the direct photolysis and the reaction with HO[•] radicals, obtaining a quite good agreement between model predictions and field data. Therefore, direct photolysis and HO[•] reaction can be important degradation pathways for imazethapyr in paddy water. DOM inhibits the phototransformation of imazethapyr because of HO[•] scavenging and of the screening of incident sunlight, which reduces the HO[•] formation rate from nitrate and nitrite and prevents light absorption by the herbicide. A similar behaviour has been found in previous works (Elazzouzi et al., 2002; Ramezani et al., 2008; Espy et al., 2011). However, by trying to model the inhibition effect of DOM reported by Espy et al. (2011), we found evidence that ³CDOM* could possibly sensitise the photodegradation of imazethapyr, and that 10⁸ L mol⁻¹ s⁻¹ could be a reasonable upper limit for the second-order rate constant of the reaction between the herbicide and ³CDOM* (a likely value could be around 10⁷ L mol⁻¹ s⁻¹). The consideration of the ³CDOM* reaction even slightly improved the agreement between the modelled imazethapyr lifetime in paddy water and the literature findings.

Although the HO[•] and ³CDOM* reactions can have a non-negligible role in imazethapyr photodegradation, respectively at low and high DOC levels, direct photolysis is a key degradation pathway. Furthermore, by assessing the toxicity of the transformation by-products by means of the ECOSAR V2.0 software, we found that the direct photolysis could be of environmental concern because it yields toxic intermediates. However, to better understand the imazethapyr photochemical

fate in paddy water, further studies should be carried out to experimentally assess: (i) the reactivity of imazethapyr toward $^3\text{CDOM}^*$, singlet oxygen (a photoreactive intermediate that could also be important in the DOM-rich rice-field waters) and the carbonate radicals; (ii) the actual toxicity of the direct-photolysis by-products, as well as of those arising from indirect photochemistry, and (iii) their formation yields.

Acknowledgements

LC acknowledges Compagnia di San Paolo (Torino, Italy) for financially supporting his PhD fellowship.

Conflict of interest

None

References

Al Housari, F., Vione, D., Chiron, S., Barbati, S., 2010. Reactive photoinduced species in estuarine waters. Characterization of hydroxyl radical, singlet oxygen and dissolved organic matter triplet state in natural oxidation processes. *Photochem. Photobiol. Sci.* 9, 78-86. DOI: 10.1039/B9PP00030E.

Appiani, E., McNeill, K., 2015. Photochemical Production of Singlet Oxygen from Particulate Organic Matter. *Environ. Sci. Technol.* 49, 6, 3514-3522. DOI: 10.1021/es505712e.

Armbrust, K. L., 2000. Pesticide hydroxyl radical rate constants: Measurements and estimates of their importance in aquatic environments. *Environ Toxicol Chem* 19, 2175-2180. DOI: 10.1002/etc.5620190905.

Avila, L. A., Massey, J. H., Senseman, S. A., Armbrust, K. L., Lancaster, S. R., Mccauley, G. N., Chandler, J. M., 2006. Imazethapyr Aqueous Photolysis, Reaction Quantum Yield, and Hydroxyl Radical Rate Constant. *J Agr Food Chem* 54, 2635-2639. DOI: 10.1021/jf052214b.

Barreiros, L., Manaia, C. M., Nunes, O. C., 2011. Bacterial diversity and bioaugmentation in floodwater of a paddy field in the presence of the herbicide molinate. *Biodegradation* 22, 445-461. DOI: 10.1007/s10532-010-9417-1.

Battaglin, W. A., Furlong, E. T., Burkhardt, M. R., Peter, C. J., 2000. Occurrence of sulfonylurea, sulfonamide, imidazolinone, and other herbicides in rivers, reservoirs and ground water in the Midwestern United States, 1998. *Sci Tot Environ* 248, 123-133. DOI: 10.1016/S0048-9697(99)00536-7.

Beretvas, M. K., Hassett, J. P., Burns, S. E., Basford, T. M., 2000. Modeling the photolysis of ammonium dinitramide in natural waters. *Environ Toxicol Chem* 19, 2661-2665. DOI: 10.1002/etc.5620191107.

Bianco, A., Fabbri, D., Minella, M., Brigante, M., Mailhot, G., Maurino, V., Minero, C., Vione, D., 2015. New insights into the environmental photochemistry of 5-chloro-2-(2,4-dichlorophenoxy)phenol (triclosan): Reconsidering the importance of indirect photoreactions. *Water Res.* 72, 271-280. DOI: 10.1016/j.watres.2014.07.036.

Bodrato, M., Vione, D., 2014. APEX (Aqueous Photochemistry of Environmentally occurring Xenobiotics): A free software tool to predict the kinetics of photochemical processes in surface waters. *Environ Sci-Proc Imp* 16, 732-740. DOI: 10.1039/C3EM00541K.

Burrows, H. D., Canle L, M., Santaballa, J. A., Steenken, S., 2002. Reaction pathways and mechanisms of photodegradation of pesticides. *J Photoc Photobio B* 67, 71-108. DOI: 10.1016/S1011-1344(02)00277-4.

Buxton, G. V., Greenstock, C. L., Helman, W. P., Ross, A. B., 1988. Critical review of rate constants for reactions of hydrated electrons, hydrogen atoms and hydroxyl radicals ($\bullet\text{OH}/\text{O}^-\bullet$) in aqueous solution. *J Phys Chem Ref Data* 17, 513-886. DOI: 10.1063/1.555805.

Canonica, S., Kohn, T., Mac, M., Real, F. J., Wirz, J., von Gunten, U., 2005. Photosensitizer Method to Determine Rate Constants for the Reaction of Carbonate Radical with Organic Compounds. *Environ. Sci. Technol.* 39, 9182–9188. DOI: 10.1021/es051236b.

Canonica, S., Laubscher, H. U., 2008. Inhibitory effect of dissolved organic matter on triplet-induced oxidation of aquatic contaminants. *Photochem. Photobiol. Sci.* 7, 547–551. DOI: 10.1039/b719982a.

Carena, L., Vione, D., 2017. A Model Study of the Photochemical Fate of As(III) in Paddy-Water. *Molecules* 22, 445. DOI: 10.3390/molecules22030445.

Carena, L., Minella, M., Barsotti, F., Brigante, M., Milan, M., Ferrero, A., Berto, S., Minero, C., Vione, D., 2017. Phototransformation of the herbicide propanil in paddy field water. *Environ Sci Technol* 51, 2695–2704. DOI: 10.1021/acs.est.6b05053.

Christiansen, A., Peterson, A., Anderson, S. C., Lass, R., Johnson, M., Nienow, A. M., 2015. Analysis of the Photodegradation of the Imidazolinone Herbicides Imazamox, Imazapic, Imazaquin, and Imazamethabenz-methyl in Aqueous Solution. *J. Agric. Food Chem.* 63, 10768-10777. DOI: 10.1021/acs.jafc.5b04663.

Elazzouzi, M., Mekkaoui, M., Zaza, S., El Madani, M., Zrineh, A., Chovelon, J. M., 2002 Abiotic Degradation of Imazethapyr in Aqueous Solution. *J Environ Sci Heal B* 37, 445-451. DOI: 10.1081/PFC-120014874.

Espy, R., Pelton, E., Opseth, A., Kasprisin, J., Nienow, A. M., 2011. Photodegradation of the Herbicide Imazethapyr in Aqueous Solution: Effects of Wavelength, pH, and Natural Organic Matter (NOM) and Analysis of Photoproducts. *J. Agric. Food Chem.* 59, 13, 7277-7285. DOI: 10.1021/jf200573g.

Fenner, K., Canonica, S., Wackett, L. P., Elsner, M., 2013. Evaluating Pesticide Degradation in

the Environment: Blind Spots and Emerging Opportunities. *Science* 341, 752-758. DOI: 10.1126/science.1236281.

Frank, R. A., Sanderson, H., Kavanagh, R., Burnison, B. K., Headley, J. V., Solomon, K. R., 2010. Use of a (Quantitative) Structure–Activity Relationship [(Q)Sar] Model to Predict the Toxicity of Naphthenic Acids. *J Toxicol Env Heal A* 73, 319 – 329. DOI: 10.1080/15287390903421235.

Haag, W. R., Hoigné, J., 1986. Singlet oxygen in surface waters. 3. Photochemical formation and steady-state concentrations in various types of waters. *Environ. Sci. Technol.* 20, 4, 341-348. DOI: 10.1021/es00146a005.

Harir, M., Frommberger, M., Gaspar, A., Martens, D., Kettrup, A., El Azzouzi, M., Schmitt-Kopplin, Ph., 2007. Characterization of imazamox degradation by-products by using liquid chromatography mass spectrometry and high-resolution Fourier transform ion cyclotron resonance mass spectrometry. *Anal Bioanal Chem* 389, 1459–1467. DOI 10.1007/s00216-007-1343-7.

Huang, J., Mabury, S. A., 2000. The role of carbonate radical in limiting the persistence of sulfur-containing chemicals in sunlit natural waters. *Chemosphere* 41, 1775-1782. DOI: 10.1016/S0045-6535(00)00042-4.

Kaloumenos, N. S., Capote, N., Aguado, A., Eleftherohorinos, I. G., 2013. Red rice (*Oryza sativa*) cross-resistance to imidazolinone herbicides used in resistant rice cultivars grown in northern Greece. *Pestic Biochem Phys* 105, 177-183. DOI: 10.1016/j.pestbp.2013.01.008.

Liu, Y., He, X., Duan, X., Fu, Y., Fatta-Kassinos, D., Dionysiou, D. D., 2016. Significant role of UV and carbonate radical on the degradation of oxytetracycline in UV-AOPs: Kinetics and mechanism. *Water Res* 95, 195-204. DOI: 10.1016/j.watres.2016.03.011.

Lonhienne, T., Garcia, M. D., Pierens, G., Mobli, M., Nouwens, A., Luke W. Guddat, L. W., 2018. Mechanism of inhibition of AHAS by herbicides. *P Natl Acad Sci USA* 115, E1945-E1954. DOI: 10.1073/pnas.1714392115.

Mabury, S. A., Crosby, D. G., 1996. Pesticide Reactivity toward Hydroxyl and Its Relationship to Field Persistence. *J. Agric. Food Chem.* 44, 1920–1924. DOI: 10.1021/jf950423y.

Mack, J., Bolton, J. R., 1999. Photochemistry of nitrite and nitrate in aqueous solution: a review. *J Photoch Photobio A* 128, 1–13. DOI: 10.1016/S1010-6030(99)00155-0.

Martini, L. F. D., Mezzomo, R. F., Avila, L. A., Massey, J. H., Marchesan, E., Zanella, R., Peixoto, S. C., Refatti, J. P., Cassol, G. V., Marques, M., 2013. Imazethapyr and imazapic runoff under continuous and intermittent irrigation of paddy rice. *Agr Water Manage* 125, 26-34. DOI: 10.1016/j.agwat.2013.04.005.

Mayo-Bean, K., Moran, K., Meylan, B., Ranslow, P., 2012. Methodology Document for the ECOlogical Structure-Activity Relationship Model (ECOSAR) Class Program. US-EPA, Washington DC, 46 pp.

McNeill, K., Canonica, S., 2016. Triplet state dissolved organic matter in aquatic photochemistry: reaction mechanisms, substrate scope, and photophysical properties. *Environ. Sci.: Processes Impacts* 18, 1381-1399. DOI: 10.1039/c6em00408c.

Milan, M., Ferrero, A., Fogliatto, S., De Palo, F., Vidotto, F., 2017. Imazamox dissipation in two rice management systems. *J Agr Sci* 155, 431-443. DOI: 10.1017/S0021859616000447.

Minella, M., Rapa, L., Carena, L., Pazzi, M., Maurino, V., Minero, C., Brigante, M., Vione, D., 2018. Experimental methodology to measure the reaction rate constants of processes sensitised by the triplet state of 4-carboxybenzophenone as proxy of the triplet states of chromophoric dissolved organic matter, under steady-state irradiation conditions. *Environ. Sci.: Processes Impacts*. DOI: 10.1039/C8EM00155C.

Ortiz de García, S.A., Pinto Pinto, G., García-Encina, P.A., Irusta-Mata, R., 2014. Ecotoxicity and environmental risk assessment of pharmaceuticals and personal care products in aquatic environments and wastewater treatment plants. *Ecotoxicology* 23, 1517-1533. DOI: 10.1007/s10646-014-1293-8.

Quesada, A., Leganés, F., Fernández-Valiente, E., 1997. Environmental factors controlling N₂ fixation in Mediterranean rice fields. *Microb. Ecol.* 34, 39-48. DOI: 10.1007/s002489900032.

Quivet, E., Faure, R., Georges, J., Païssé, J. O., Herbreteau, B., 2004. Kinetic studies of imazapyr photolysis and characterization of the main photoproducts. *Toxicol Environ Chem* 86, 197-206. DOI: 10.1080/02772240400007054.

Quivet, E., Faure, R., Georges, J., Païssé, J. O., Herbreteau, B., Lantéri, P., 2006. Photochemical Degradation of Imazamox in Aqueous Solution: Influence of Metal Ions and Anionic Species on the Ultraviolet Photolysis. *J. Agric. Food Chem.* 54, 3641-3645. DOI: 10.1021/jf060097u.

Ramezani, M., Oliver, D. P., Kookana, R. S., Gill, G., Preston, C., 2008. Abiotic degradation (photodegradation and hydrolysis) of imidazolinone herbicides. *J Environ Sci Heal B* 43, 105-112, DOI: 10.1080/03601230701794968.

Reimche, G. B., Machado, S. L. O., Oliveira, M. A., Zanella, R., Dressler, V. L., Flores, E. M. M., Gonçalves, F. F., Donato, F. F., Nunes, M. A. G., 2015. Imazethapyr and imazapic, bispyribac-sodium and penoxsulam: Zooplankton and dissipation in subtropical rice paddy water. *Sci Total Environ* 514, 68-76, DOI: 10.1016/j.scitotenv.2015.01.055.

Remucal, C. K., 2014. The role of indirect photochemical degradation in the environmental fate of pesticides: a review. *Environ. Sci.: Processes Impacts* 16, 628-653. DOI: 10.1039/C3EM00549F.

Reuschenbach, P., Silvani, M., Dammann, M., Warnecke, D., Knacker, T., 2008. ECOSAR model performance with a large test set of industrial chemicals. *Chemosphere* 71, 1986-1995. DOI: 10.1016/j.chemosphere.2007.12.006.

Rodenburg, J., Meinke, H., Johnson, D., 2011. Challenges for weed management in African rice systems in a changing climate. *J Agr Sci* 149, 427-435. DOI: 10.1017/S0021859611000207.

Roger, P. A., 1996. Biology and management of the floodwater ecosystem in rice fields. International Rice Research Institute. P. O. Box 933, Manila 1099, Philippines, pp. 7-14.

Saito, M., Watanabe, I., 1978. Organic matter production in rice field flood water. *Soil Sci Plant Nutr* 24, 427-440. DOI:10.1080/00380768.1978.10433121.

Santos, F.M., Marchesan, E., Machado, S. L. O., Avila, L. A., Zanella, R., Gonçalves, F. F., 2008. Persistência dos herbicidas imazethapyr e clomazone em lâmina de água do arroz irrigado. *Planta Daninha* 26, 875-881. DOI: 10.1590/S0100-83582008000400019.

Scarabel, L., Cenghialta, C., Manuello, D., Sattin, M., 2012. Monitoring and Management of Imidazolinone-Resistant Red Rice (*Oryza sativa* L., var. *sylvatica*) in Clearfield® Italian Paddy Rice. *Agronomy* 2, 371-383. DOI: 10.3390/agronomy2040371.

Shivrain, V. K., Burgos, N. R., Gealy, D. R., Smith, K. L., Scott, R. C., Mauromoustakos, A., Black, H., 2009. Red rice (*Oryza sativa*) emergence characteristics and influence on rice yield at different planting dates. *Weed Sci.* 57, 94-102. DOI: 10.1614/WS-08-112.1.

Sudianto, E., Beng-Kah, S., Ting-Xiang, N., Saldain, N. E., Scott, R. C., Burgos, N. R., 2013. Clearfield® rice: Its development, success, and key challenges on a global perspective. *Crop Prot* 49, 40-51, DOI: 10.1016/j.cropro.2013.02.013.

Tan, S., Evans, R. R., Dahmer, M. L., Singh, B. K., Shaner, D. L., 2005. Imidazolinone-tolerant crops: history, current status and future. *Pest Manag Sci* 61, 246-257. DOI: 10.1002/ps.993.

Timko, S. A., Romera-Castillo, C., Jaffè, R., Cooper, W. J., 2014. Photo-reactivity of natural dissolved organic matter from fresh to marine waters in the Florida Everglades, USA. *Environ. Sci: Processes Impacts* 16, 866-878. DOI: 10.1039/C3EM00591G.

Trinh, H. T., Marcussen, H., Hansen, H. C. B., Truong, G. L., Duong, H. T., Nguyen, T. Q., Hansen, S., Strobel, B. W., 2017. Screening of inorganic and organic contaminants in floodwater in

paddy fields of Hue and Thanh Hoa in Vietnam. *Environ. Sci. Pollut. Res.* 24, 7348-7358. DOI: 10.1007/s11356-017-8433-7.

Turro, N. J., Ramamurthy, V., Cherry, W., Farneth, W., 1978. The effect of wavelength on organic photoreactions in solution. Reactions from upper excited states. *Chem. Rev.* 78, 125-145. DOI: 10.1021/cr60312a003.

Vione, D., 2014. A test of the potentialities of the APEX software (Aqueous Photochemistry of Environmentally occurring Xenobiotics). Modelling the photochemical persistence of the herbicide cycloxydim in surface waters, based on literature kinetic data. *Chemosphere* 99, 272-275. DOI: 10.1016/j.chemosphere.2013.10.078.

Vione, D., Minella, M., Maurino, V., Minero, C., 2014. Indirect photochemistry in sunlit surface waters: Photoinduced production of reactive transient species. *Chem. Eur. J.* 20, 10590–10606. DOI: 10.1002/chem.201400413.

Vione, D., Fabbri, D., Minella, M., Canonica, S., 2018. Effects of the antioxidant moieties of dissolved organic matter on triplet-sensitized phototransformation processes: Implications for the photochemical modeling of sulfadiazine. *Water Res* 128, 38-48. DOI: 10.1016/j.watres.2017.10.020.

Wenk, J., von Gunten, U., Canonica; S., 2011. Effect of Dissolved Organic Matter on the Transformation of Contaminants Induced by Excited Triplet States and the Hydroxyl Radical. *Environ. Sci. Technol.* 45, 4, 1334-1340. DOI: 10.1021/es102212t.

Wenk, J., Canonica, S., 2012. Phenolic Antioxidants Inhibit the Triplet-Induced Transformation of Anilines and Sulfonamide Antibiotics in Aqueous Solution. *Environ. Sci. Technol.* 46, 10, 5455-5462. DOI: 10.1021/es300485u.

Wei, L. N., Wu, P., Wang, F. R., Yang, H., 2015. Dissipation and Degradation Dynamics of Thifluzamide in Rice Field. *Water Air Soil Pollut* 226, 458-463. DOI: 10.1007/s11270-015-2387-5.

Xie, J., Zhao, L., Liu, K., Guo, F., Gao, L., Liu, W., 2018. Activity, toxicity, molecular docking, and environmental effects of three imidazolinone herbicides enantiomers. *Sci Total Environ* 622-623, 594-602. DOI: 10.1016/j.scitotenv.2017.11.333.

Yuan, C., Chakraborty, M., Canonica, S., Weavers, L. K., Hadad, C. M., Chin, Y. P., 2016. Isoproturon Reappearance after Photosensitized Degradation in the Presence of Triplet Ketones or Fulvic Acids. *Environ. Sci. Technol.* 50, 22, 12250-12257. DOI: 10.1021/acs.est.6b03655.

Zanella, R., Adaime, M. B., Peixoto, S. C., Friggi, C. A., Prestes, O. D., Machado, S. L. O., Marchesan, E., Avila, L. A., Primel, E. G., 2011. Herbicides Persistence in Rice Paddy Water in Southern Brazil, *Herbicides - Mechanisms and Mode of Action*, Dr. Mohammed Nagib Hasaneen (Ed.), InTech, DOI: 10.5772/32727. Available from: <https://mts.intechopen.com/books/herbicides-mechanisms-and-mode-of-action/herbicides-persistence-in-rice-paddy-water-in-southern-brazil>.